



Received 9 September 2019

Accepted 23 September 2019

Edited by L. Van Meervelt, Katholieke Universiteit Leuven, Belgium

**Keywords:** crystal structure; chloromercurate(II) salt; 4-dimethylaminopyridinium; Hirshfeld surface; fingerprint plots; hybrid compound.

**CCDC reference:** 1911692

**Supporting information:** this article has supporting information at journals.iucr.org/e

# Crystal structure, Hirshfeld surface analysis and physicochemical characterization of bis[4-(dimethylamino)pyridinium] di- $\mu$ -chlorido-bis[di-chloridomercurate(II)]

Fatma Garci,<sup>a</sup> Hela Ferjani,<sup>b</sup> Hammouda Chebbi,<sup>a\*</sup> Mariem Ben Jomaa<sup>a</sup> and Mohamed Faouzi Zid<sup>a</sup>

<sup>a</sup>University of Tunis El Manar, Faculty of Sciences of Tunis, Laboratory of Materials, Crystal Chemistry and Applied Thermodynamics, 2092 El Manar II, Tunis, Tunisia, and <sup>b</sup>Chemistry Department, College of Science, IMSIU (Imam Mohammad Ibn Saud Islamic University), Riyadh 11623, Kingdom of Saudi Arabia. \*Correspondence e-mail: chebhamouda@yahoo.fr

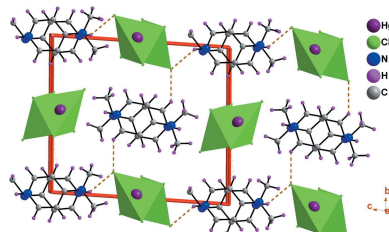
The title molecular salt,  $(C_7H_{11}N_2)_2[Hg_2Cl_6]$ , crystallizes with two 4-(dimethylamino)pyridinium cations (*A* and *B*) and two half hexachloridodimercurate(II) anions in the asymmetric unit. The organic cations exhibit essentially the same features with an almost planar pyridyl ring (r.m.s. deviations of 0.0028 and 0.0109 Å), which forms an inclined dihedral angle with the dimethylamino group [3.06 (1) and 1.61 (1)°, respectively]. The dimethylamino groups in the two cations are planar, and the C–N bond lengths are shorter than that in 4-(dimethylamino)pyridine. In the crystal, mixed cation–anion layers lying parallel to the (010) plane are formed through N–H···Cl hydrogen bonds and adjacent layers are linked by C–H···Cl hydrogen bonds, forming a three-dimensional network. The analyses of the calculated Hirshfeld surfaces confirm the relevance of the above intermolecular interactions, but also serve to further differentiate the weaker intermolecular interactions formed by the organic cations and inorganic anions, such as  $\pi$ – $\pi$  and Cl···Cl interactions. The powder XRD data confirms the phase purity of the crystalline sample. Furthermore, the vibrational absorption bands were identified by IR spectroscopy and the optical properties were studied by using optical UV–visible absorption spectroscopy.

## 1. Chemical context

Hybrid organic–inorganic materials have been widely studied in recent years for their promising applications in different fields, including catalysis, magnetism and optics and for their luminescence properties (Clément *et al.*, 1994; Rabu *et al.*, 2001; Hu *et al.*, 2003; Morris *et al.*, 2008). However, owing to the confinement of the inorganic layers, the organic cations have to possess the right ionic bond and steric hindrance, as well as hydrogen bonds, to fit the coordination environment provided by the inorganic framework for stabilization of these organic–inorganic hybrid systems.

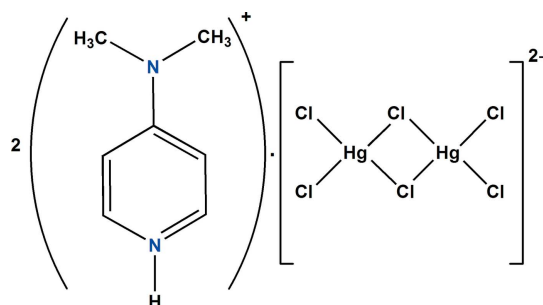
Hybrids based on mercury have been synthesized and characterized with simple, different techniques, thanks to their self-assembling character (Mitzi *et al.*, 2001) and are very interesting both for fundamental physics exploration such as electronic confinement (Wei *et al.*, 2015) or as low-dimensional magnetic systems (Fersi *et al.*, 2015) and diversify the field of technological applications.

A number of chloromercurate(II) complexes have been shown to exhibit ferroelectric behaviour (Mitsui & Nakamura, 1990) and interest has focused on the mechanism of the



OPEN ACCESS

ferroelectric–paraelectric phase transition (White, 1963; Körfer *et al.*, 1988; Jiang *et al.*, 1995; Liesegang *et al.*, 1995) for which structural information is crucial. In addition, the ability of the anions in this class of compounds to exhibit a wide range of geometry, stoichiometry and connectivity has long been known (Grdenic, 1965). This flexibility is a result of the large volume and spherical charge distribution of the  $\text{Hg}^{2+}$  ion, which are a consequence of the filled 4f and 5d electron shells. Moreover, organic–inorganic materials with pyridine and its derivatives as template agents have led to the preparation of some materials with interesting physical properties (Aakeröy *et al.*, 2000; Prince *et al.*, 2003) and biological activities (Bossert *et al.*, 1981; Wang *et al.*, 1989).



As part of our continuing investigation of new hybrid compounds containing an organic cation and an inorganic anion such as  $\text{CrO}_4^{2-}$  (Chebbi *et al.*, 2000; Chebbi & Driss, 2001, 2002a,b, 2004),  $\text{Cr}_2\text{O}_7^{2-}$  (Chebbi *et al.*, 2016, Ben Smail *et al.*, 2017),  $\text{NO}_3^-$  (Chebbi *et al.*, 2014, 2018) and  $\text{ClO}_4^-$  (Chebbi *et al.*, 2017; Ben Jomaa *et al.*, 2018), we report in this work the crystal structure, the Hirshfeld surface analysis and the physicochemical characterization of a new organic chloromercurate(II),  $(\text{C}_7\text{H}_{11}\text{N}_2)_2[\text{Hg}_2\text{Cl}_6]$  (I).

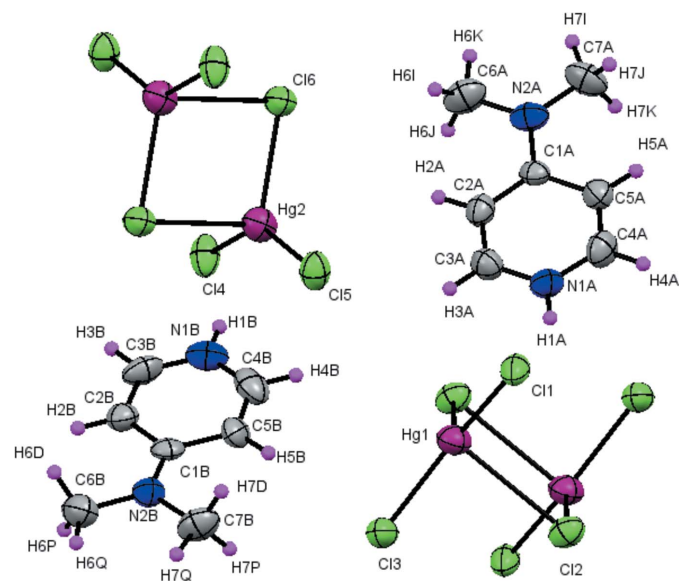


**Figure 1**

The molecular structure of (I). Atomic displacement parameters for the non-H atoms are drawn at the 50% probability level. Unlabelled atoms are related to labelled ones by the symmetry operation  $-x + 1, -y, -z + 2$ .

## 2. Structural commentary

The asymmetric unit of the title compound comprises two 4-(dimethylamino)pyridinium cations (*A* and *B*), and two half  $[\text{Hg}_2\text{Cl}_6]^{2-}$  anions (Fig. 1). The two independent  $[\text{Hg}_2(1,2)\text{Cl}_6]^{2-}$  anions are found to adopt a centrosymmetric arrangement with terminal  $\text{Cl}1-\text{Hg}1-\text{Cl}3$  and  $\text{Cl}4-\text{Hg}2-\text{Cl}5$  angles of  $141.4(1)^\circ$  and  $141.7(1)^\circ$  respectively. Each anion appears to be a distorted edge-shared bitetrahedron, similar to that reported by Larock *et al.* (1987), with its center of mass coincident with a crystallographic center of symmetry. The two independent  $\text{Hg}\cdots\text{Cl}$  bridging distances are  $2.539(2)$  and  $2.542(2)$  Å, leading to a slightly asymmetric bridging system as has been found in most structures containing the  $[\text{Hg}_2\text{Cl}_6]^{2-}$  moiety (Linden *et al.*, 1999; Zabel *et al.*, 2008). In each anion, the two terminal  $\text{Hg}-\text{Cl}$  bonds are quite short [ $\text{Hg}1-\text{Cl}1 = 2.371(2)$  and  $\text{Hg}1-\text{Cl}3 = 2.380(2)$  Å,  $\text{Hg}2-\text{Cl}4 = 2.367(3)$  and  $\text{Hg}2-\text{Cl}5 = 2.392(2)$  Å] with a  $\text{Cl}1-\text{Hg}1-\text{Cl}2$  and  $\text{Cl}4-\text{Hg}2-\text{Cl}6$  angles of  $112.01(9)$  and  $112.72(10)^\circ$ , respectively. Assessment of the organic geometrical features shows that they exhibit essentially the same features with an almost planar pyridyl ring (r.m.s. deviation =  $0.0028$  and  $0.0109$  Å for  $\text{C}1\text{A}-\text{C}5\text{A}/\text{N}1\text{A}$  and  $\text{C}1\text{B}-\text{C}5\text{B}/\text{N}1\text{B}$ , respectively), which forms an inclined dihedral angle with the dimethylamino group [ $3.06(1)$  and  $1.61(1)^\circ$ , respectively]. The dimethylamino groups in the two cations are planar and the  $\text{C}-\text{N}$  bond lengths [ $1.357(11)$  Å for *A* and  $1.326(11)$  Å for *B*] are shorter than that in 4-dimethylaminopyridine [ $1.367(2)$  Å; Ohms & Guth, 1984]. These findings indicate the presence of strong conjugation between the dimethylamino group and the pyridine ring. The  $\text{C}3\text{A}-\text{N}1\text{A}-\text{C}4\text{A}$  [ $121.2(8)^\circ$ ] and  $\text{C}3\text{B}-\text{N}1\text{B}-\text{C}4\text{B}$  [ $119.8(9)^\circ$ ] bond angles are wider than that in pyridine ( $116.94^\circ$ ; Sørensen *et al.*, 1974), which indicates that the pyridine ring N atom is protonated. Examination of the  $\text{C}-\text{C}(\text{N})$  distances and  $\text{C}-\text{C}-\text{C}(\text{N})$ ,  $\text{C}-\text{N}-\text{C}$  angles in the 4-(dimethylamino)pyridinium dications (*A* and *B*) shows no significant difference from those obtained in other organic materials associated with the same organic groups (Chao *et al.*, 1977; Mustaqim *et al.*, 2005).

The experimental powder X-ray diffraction pattern of the title compound,  $(\text{C}_7\text{H}_{11}\text{N}_2)_2[\text{Hg}_2\text{Cl}_6]$  is in good agreement with that simulated (Fig. 2). This indicates the purity of the synthesized product and confirms the crystal data used.

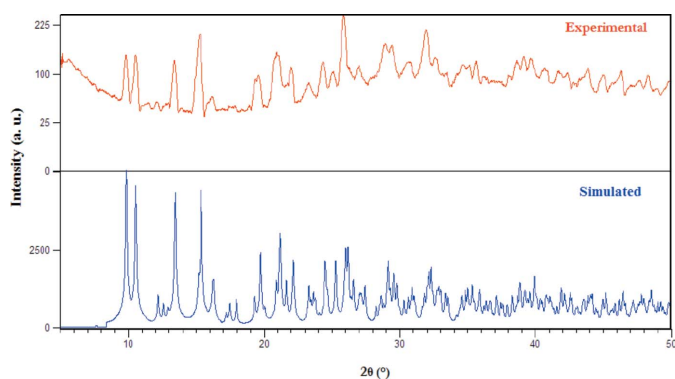


**Figure 2**

Experimental and simulated powder XRD patterns of (I).

**Table 1**  
Hydrogen-bond geometry ( $\text{\AA}$ ,  $^\circ$ ).

$D-\text{H}\cdots A$	$D-\text{H}$	$\text{H}\cdots A$	$D\cdots A$	$D-\text{H}\cdots A$
N1A—H1A $\cdots$ Cl3	0.86	2.54	3.239 (8)	140
N1B—H1B $\cdots$ Cl5	0.86	2.46	3.195 (10)	145
C2B—H2B $\cdots$ Cl1 <sup>i</sup>	0.93	2.82	3.634 (11)	147
C3A—H3A $\cdots$ Cl5	0.93	2.75	3.485 (11)	136

Symmetry code: (i)  $-x + 1, -y, -z + 2$ .

### 3. Supramolecular features

In the crystal structure, mixed cation–anion layers lying parallel to the (010) plane are formed through  $\text{N}-\text{H}\cdots\text{Cl}$  hydrogen bonds and adjacent layers are linked by  $\text{C}-\text{H}\cdots\text{Cl}$  hydrogen bonds, forming a three-dimensional network (Table 1, Fig. 3). A mixed layer is formed by alternating of organic and inorganic columns parallel to the [100] direction

(Fig. 4). The cations (*A* or *B*) interact via offset face-to-face  $\pi$ – $\pi$  stacking interactions, leading to two types of organic columns formed by the cations (*A* or *B*) with centroid–centroid distances of 3.698 (2) and 3.982 (2)  $\text{\AA}$ , respectively (Fig. 5) (Janiak, 2000; Ben Moussa *et al.*, 2018). Similarly, the hexachloridodimercurate(II) anions are dispersed parallel to the *a* axis whose cohesion is ensured by  $\text{Cl}\cdots\text{Cl}$  [3.652 (6)  $\text{\AA}$ ] and  $\text{Hg}\cdots\text{Cl}$  [3.167 (7)  $\text{\AA}$ ] weak interactions (Sumanesh *et al.*, 2016; Ben Moussa *et al.*, 2019*a,b*; Fig. 6).

### 4. Vibrational study

The obtained FT–IR spectrum for the studied hexachloridodimercurate(II) salt is depicted in Fig. 7. Detailed assignment of all bands observed in the infrared spectrum of the 4-(dimethylamino)pyridinium cation in the title compound is based on the comparison with other compounds associated to the same cation (Koleva *et al.*, 2008; Hu *et al.*, 2012). In the region of high frequencies, the bands at 3243, 3130, 3100, 2959  $\text{cm}^{-1}$  are due to the stretching vibrations of the  $\text{N}-\text{H}$  and  $\text{C}-\text{H}$  bonds. The band at 1646  $\text{cm}^{-1}$  is assigned to the  $\text{N}-\text{H}$  bending mode. The bands at 1557 and 1445  $\text{cm}^{-1}$  are attributed to the  $\text{C}=\text{C}$  and  $\text{C}=\text{N}$  stretching modes of the pyridine ring. The absorption band located at 1212  $\text{cm}^{-1}$  corresponds to the  $\nu(\text{C}=\text{N})$  and  $\nu(\text{C}=\text{C})$  modes. The band at 1056  $\text{cm}^{-1}$  can be attributed to the  $\delta(\text{C}=\text{C})$  mode. The remaining bands in the

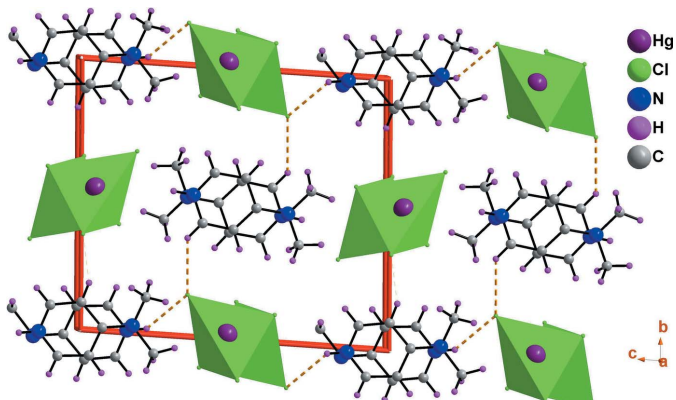


**Figure 3**

Structure of (I) viewed along the *a* axis showing the succession of mixed layers parallel to the (010) plane. The orange dotted lines indicate hydrogen bonds.

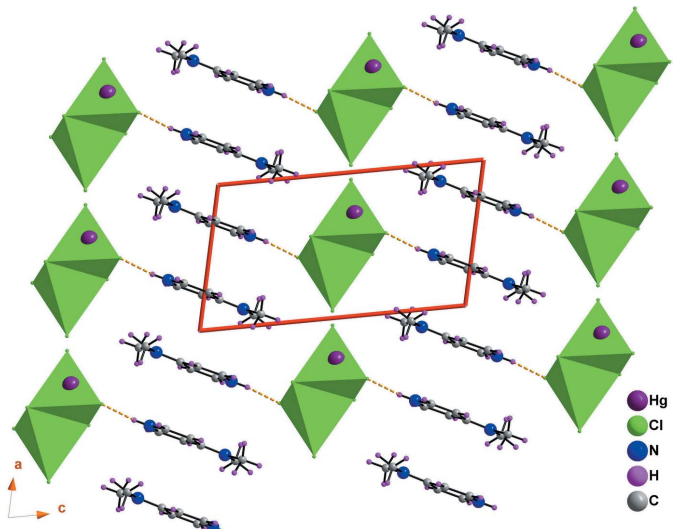


**Figure 4**

A view of the supramolecular mixed layer in the *ac* plane of (I), showing the alternating organic and inorganic columns parallel to the [100] direction. The orange dotted lines indicate  $\text{N}-\text{H}\cdots\text{Cl}$  hydrogen bonds.

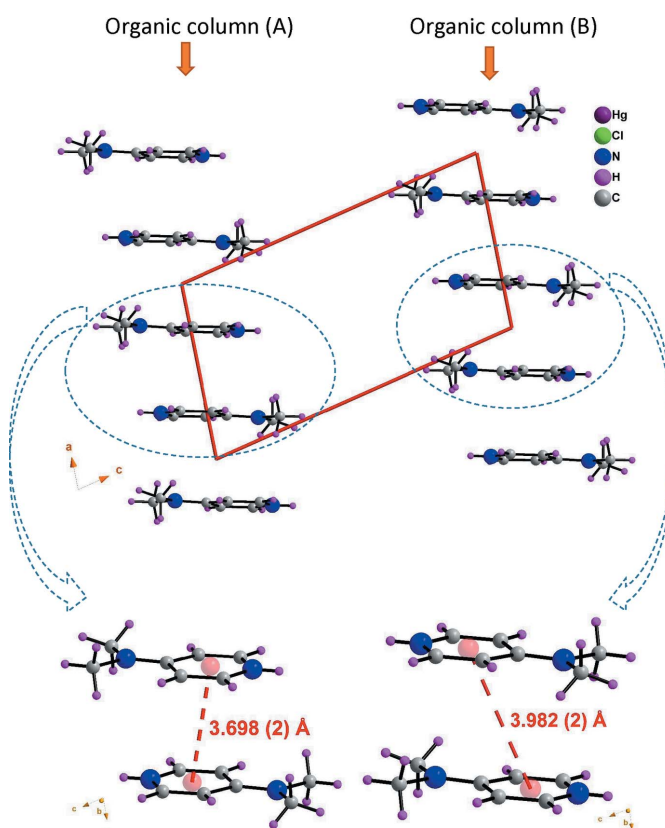


**Figure 5**

$\pi$ – $\pi$  stacking interactions between the nearest aromatic organic cation neighbors into two types of organic columns (*A* or *B*).

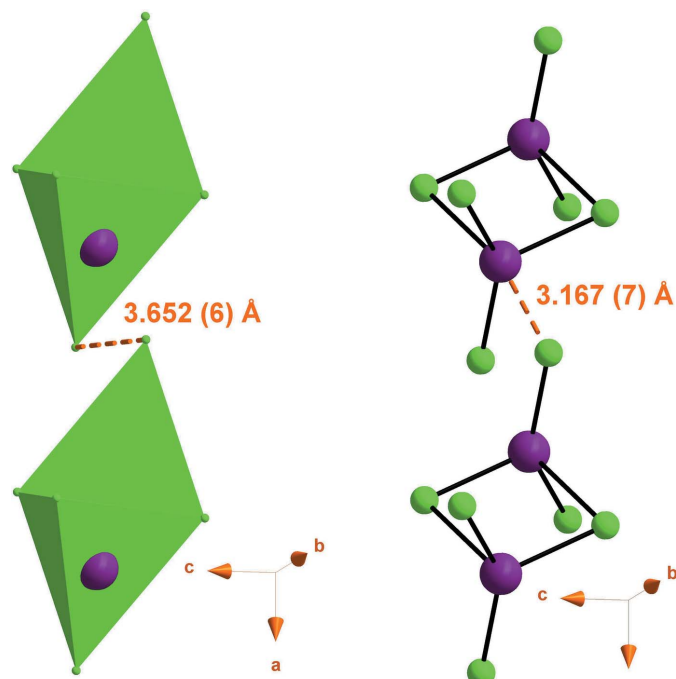


**Figure 6**  
Cl···Cl and Hg···Cl interactions between hexachloridodimercurate(II) anions dispersed parallel to the *a* axis in the inorganic column.

range 1000 to 500 cm<sup>-1</sup> are assigned to  $\gamma(\text{C}-\text{C})$ ,  $\gamma(\text{C}-\text{H})$  and  $\gamma(\text{C}-\text{N})$  out-of-plane bending modes.

## 5. Optical properties and frontier molecular orbitals

Optical absorption (OA) measurement of the title compound was performed at ambient temperature in an ethanol solution ( $10^{-4} M$ ). As shown in Fig. 8, the OA spectrum exhibits two distinct absorption bands around 213 and 278 nm assigned to the  $\pi \rightarrow \pi^*$  absorption bands of the 4-(dimethylamino)-pyridinium cations. Thus, the experimental band-gap energy obtained from the absorption edge wavelength is about 3.98 eV. This band-gap value indicates that the grown crystal

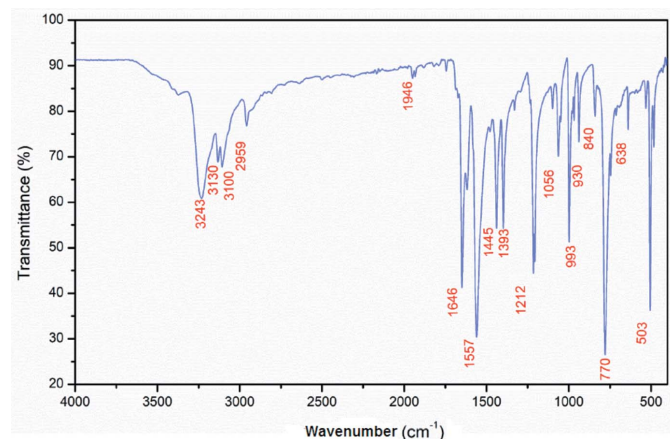


**Figure 7**  
Infrared spectrum of (I).

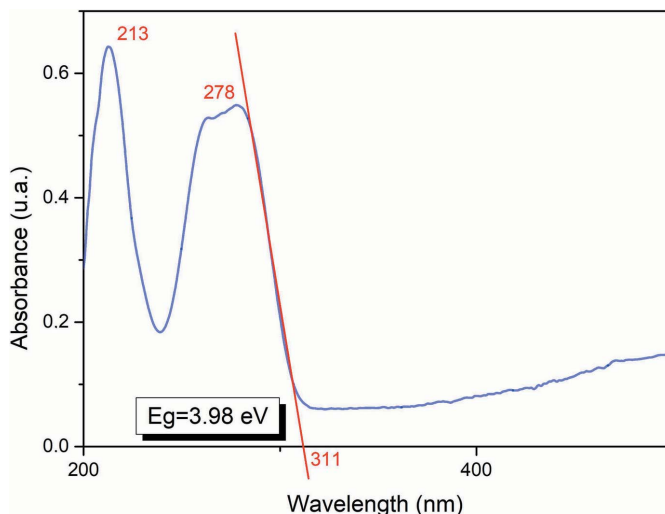


**Figure 8**  
UV-vis spectrum of (I). The inset shows the experimental energy band gap obtained from the absorption edge wavelength.

exhibits semiconductor behavior (Rosencher & Vinter, 2002). The highest occupied molecular orbital (HOMO) and the lowest unoccupied molecular orbital (LUMO), known as frontier orbitals, obtained with a B3LYP/6-311G+(d,p) [H, C, N, Cl]-LANL2DZ [Hg] level calculation are illustrated in Fig. 9. The HOMO is mainly delocalized at the pyridine ring system. After excitation, the charge is localized on the hexachloridodimercurate(II) moieties, as depicted in the LUMO. The calculated HOMO-LUMO energy gap (4.26 eV) is shifted from the experimental value, which may be attributed to solvent effects, compared to the gas-phase calculation.

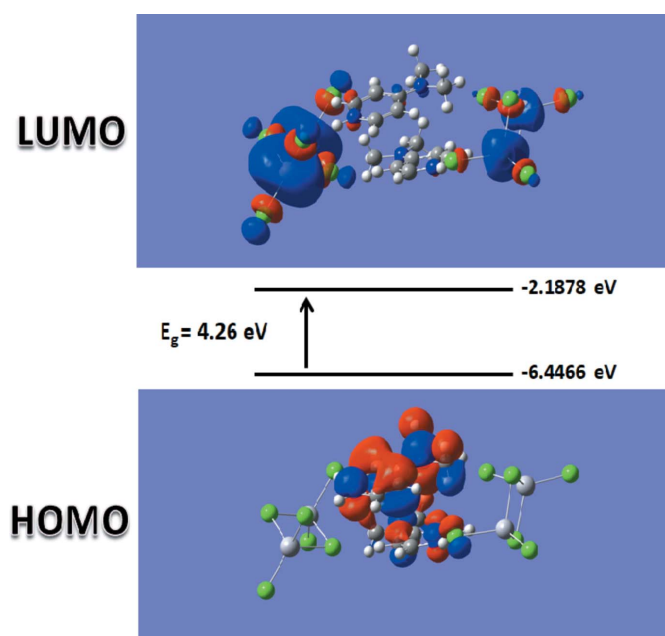


**Figure 9**  
HOMO-LUMO molecular orbitals showing the ground to excited state electronic transitions for (I).

## 6. Hirshfeld surface analysis

A Hirshfeld surface analysis (Spackman & Jayatilaka, 2009) and the associated two-dimensional fingerprint plots (McKinnon *et al.*, 2007) were performed with *Crystal-Explorer17* (Turner *et al.*, 2017) to investigate the intermolecular interactions in the title compound. Fig. 10*a* illustrates the Hirshfeld surface mapped over  $d_{\text{norm}}$ , which was plotted with a colour scale of  $-0.211$  to  $1.132$  a.u. with a standard (high) surface resolution. The red spots highlight the interatomic contacts including the  $\text{N} - \text{H} \cdots \text{Cl}$  and  $\text{C} - \text{H} \cdots \text{Cl}$  hydrogen bonds.

The shape-index of the Hirshfeld surface is a tool to visualize the  $\pi - \pi$  stacking by the presence of adjacent red and blue triangles; if there are no adjacent red and/or blue triangles, then there are no  $\pi - \pi$  interactions. Fig. 10*b* clearly suggests that  $\pi - \pi$  interactions are present in the title hexachloridodimercuroate(II) salt.

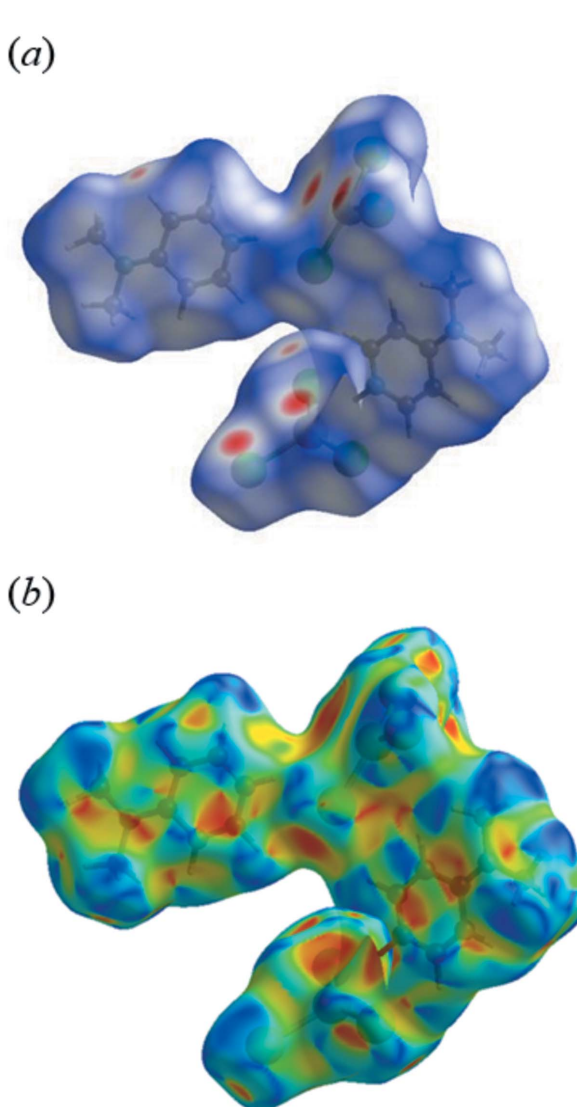


**Figure 10**  
View of the Hirshfeld surfaces for (I) mapped over (a)  $d_{\text{norm}}$  and (b) shape-index, displaying the intermolecular interactions.

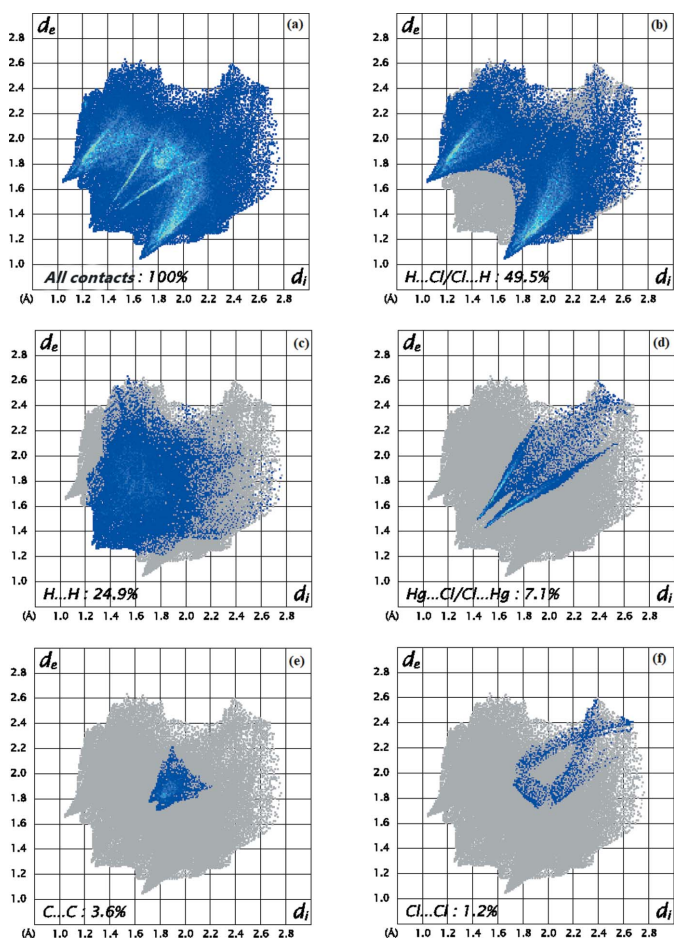


**Figure 11**  
Full two-dimensional fingerprint plots for (I), showing (a) all interactions, and delineated into (b)  $\text{H} \cdots \text{Cl}/\text{Cl} \cdots \text{H}$ , (c)  $\text{H} \cdots \text{H}$ , (d)  $\text{Hg} \cdots \text{Cl}/\text{Cl} \cdots \text{Hg}$ , (e)  $\text{C} \cdots \text{C}$  and (f)  $\text{Cl} \cdots \text{Cl}$  interactions. The  $d_i$  and  $d_e$  values are the closest internal and external distances (in Å) from a given point on the Hirshfeld surface.

Fig. 11*a* shows the two-dimensional fingerprint of all contacts contributing to the Hirshfeld surface. In Fig. 11*b*, with two symmetrical wings on the left and right sides illustrate the  $\text{H} \cdots \text{Cl}/\text{Cl} \cdots \text{H}$  interactions with a contribution of 49.5%. Fig. 11*c* illustrates the two-dimensional fingerprint plot of ( $d_i$ ,  $d_e$ ) points related to  $\text{H} \cdots \text{H}$  contacts, which represent a 24.9% contribution. Furthermore, there are  $\text{Hg} \cdots \text{Cl}/\text{Cl} \cdots \text{Hg}$

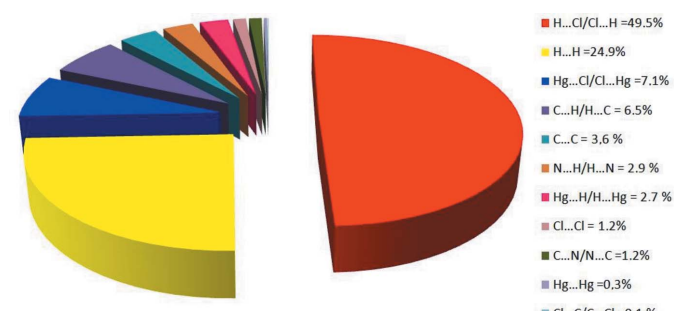


**Figure 12**  
Relative contribution (%) of various intermolecular interactions to the Hirshfeld surface area.

**Table 2**  
Experimental details.

Crystal data	
Chemical formula	(C <sub>7</sub> H <sub>11</sub> N <sub>2</sub> ) <sub>2</sub> [Hg <sub>2</sub> Cl <sub>6</sub> ]
M <sub>r</sub>	860.23
Crystal system, space group	Triclinic, P <bar{1}< td=""></bar{1}<>
Temperature (K)	293
a, b, c (Å)	7.6558 (3), 11.8961 (5), 13.5853 (4)
α, β, γ (°)	82.950 (3), 76.072 (3), 76.339 (4)
V (Å <sup>3</sup> )	1164.07 (8)
Z	2
Radiation type	Mo K $\alpha$
μ (mm <sup>-1</sup> )	13.87
Crystal size (mm)	0.72 × 0.24 × 0.18
Data collection	
Diffractometer	Enraf–Nonius CAD-4
Absorption correction	ψ scan (North <i>et al.</i> , 1968)
T <sub>min</sub> , T <sub>max</sub>	0.53, 0.99
No. of measured, independent and observed [I > 2σ(I)] reflections	7139, 5875, 3913
R <sub>int</sub>	0.040
(sin θ/λ) <sub>max</sub> (Å <sup>-1</sup> )	0.671
Refinement	
R[F <sup>2</sup> > 2σ(F <sup>2</sup> )], wR(F <sup>2</sup> ), S	0.055, 0.153, 1.03
No. of reflections	5875
No. of parameters	236
H-atom treatment	H-atom parameters constrained
Δρ <sub>max</sub> , Δρ <sub>min</sub> (e Å <sup>-3</sup> )	3.41, -3.00

Computer programs: CAD-4 EXPRESS (Duisenberg, 1992; Maciček & Yordanov, 1992), XCAD4 (Harms & Wocadlo, 1995), SHELLXT2018 (Sheldrick, 2015a), SHELLXL2018 (Sheldrick, 2015b), DIAMOND (Brandenburg, 2006), Mercury (Macrae *et al.*, 2006), WinGX (Farrugia, 2012) and publCIF (Westrip, 2010).

(7.1%; Fig. 11d), C···C (3.6%; Fig. 11e) and Cl···Cl (1.2%; Fig. 11f) contacts. Fig. 12 shows the percentage contributions of the various contacts in the title structure.

## 7. Synthesis and crystallization

The title compound was synthesized by dissolving 2 mmol (241 mg) of 4-dimethylaminopyridine 98% (Sigma–Aldrich) in an HCl 36–38% (Sigma–Aldrich) aqueous solution and 1 mmol (273 mg) of mercury(II) chloride HgCl<sub>2</sub> (Merck) in ethanol in a molar ratio of 2:1. The mixture was then stirred for 2 h. The resulting aqueous solution was filtered and then evaporated at room temperature, which finally led to the growth of parallelepipedic colourless crystals after one day.

## 8. Refinement

Crystal data, data collection and structure refinement details are summarized in Table 2. H atoms were placed in calculated positions, with N–H = 0.86 Å and C–H = 0.93 or 0.96 Å. U<sub>iso</sub>(H) values were constrained to be 1.5U<sub>eq</sub> of the carrier atom for methyl H atoms, and 1.2U<sub>eq</sub> for the remaining H atoms. The (111) and (121) reflections were omitted owing to bad disagreement.

## References

- Aakeröy, C. B., Beatty, A. M., Leinen, D. S. & Lorimer, K. R. (2000). *Chem. Commun.* pp. 935–936.
- Ben Jomaa, M., Chebbi, H., Fakhar Bourguiba, N. & Zid, M. F. (2018). *Acta Cryst. E* **74**, 91–97.
- Moussa, Ben O., Chebbi, H., Arfaoui, Y., Falvello, L. R., Tomas, M. & Zid, M. F. (2019b). *J. Mol. Struct.* **1195**, 344–354.
- Ben Moussa, O., Chebbi, H. & Zid, M. F. (2018). *Acta Cryst. E* **74**, 436–440.
- Ben Moussa, O., Chebbi, H. & Zid, M. F. (2019a). *J. Mol. Struct.* **1180**, 72–80.
- Ben Smail, R., Chebbi, H., Srinivasan, B. R. & Zid, M. F. (2017). *J. Struct. Chem.* **58**, 724–733.
- Bossert, F., Meyer, H. & Wehinger, E. (1981). *Angew. Chem. Int. Ed. Engl.* **20**, 762–769.
- Brandenburg, K. (2006). DIAMOND. Crystal Impact GbR, Bonn, Germany.
- Chao, M., Schempp, E. & Rosenstein, D. (1977). *Acta Cryst. B* **33**, 1820–1823.
- Chebbi, H., Ben Smail, R. & Zid, M. F. (2014). *Acta Cryst. E* **70**, o642.
- Chebbi, H., Ben Smail, R. & Zid, M. F. (2016). *J. Struct. Chem.* **57**, 632–635.
- Chebbi, H., Boumakhla, A., Zid, M. F. & Guesmi, A. (2017). *Acta Cryst. E* **73**, 1453–1457.
- Chebbi, H. & Driss, A. (2001). *Acta Cryst. C* **57**, 1369–1370.
- Chebbi, H. & Driss, A. (2002a). *Acta Cryst. E* **58**, m147–m149.
- Chebbi, H. & Driss, A. (2002b). *Acta Cryst. E* **58**, m494–m496.
- Chebbi, H. & Driss, A. (2004). *Acta Cryst. E* **60**, m904–m906.
- Chebbi, H., Hajem, A. A. & Driss, A. (2000). *Acta Cryst. C* **56**, e333–e334.
- Chebbi, H., Mezrigui, S., Ben Jomaa, M. & Zid, M. F. (2018). *Acta Cryst. E* **74**, 949–954.
- Clément, R., Lacroix, P. G., O'Hare, D. & Evans, J. (1994). *Adv. Mater.* **6**, 794–797.
- Duisenberg, A. J. M. (1992). *J. Appl. Cryst.* **25**, 92–96.
- Farrugia, L. J. (2012). *J. Appl. Cryst.* **45**, 849–854.
- Fersi, M. A., Chaabane, I., Gargouri, M. & Bulou, A. (2015). *Polyhedron*, **85**, 41–47.
- Grdenic, D. (1965). *Q. Rev. Chem. Soc.* **19**, 303–328.
- Harms, K. & Wocadlo, S. (1995). XCAD4. University of Marburg, Germany.
- Hu, A., Ngo, H. L. & Lin, W. (2003). *J. Am. Chem. Soc.* **125**, 11490–11491.
- Hu, Y. L., Lin, J. H., Han, S., Chen, W. Q., Yu, L. L., Zhou, D. D., Yin, W. T., Zuo, H. R., Zhou, J. R., Yang, L. M. & Ni, C. L. (2012). *Synth. Met.* **162**, 1024–1029.
- Janiak, C. (2000). *J. Chem. Soc. Dalton Trans.* pp. 3885–3896.
- Jiang, Z.-T., James, B. D., Liesegang, J., Tan, K. L., Gopalakrishnan, R. & Novak, I. (1995). *J. Phys. Chem. Solids*, **56**, 277–283.
- Koleva, B. B., Kolev, T., Seidel, R. W., Tsanev, T., Mayer-Figge, H., Spitteler, M. & Sheldrick, W. S. (2008). *Spectrochim. Acta A*, **71**, 695–702.
- Körfer, M., Fuess, H., Prager, M. & Zehnder, E.-J. (1988). *Ber. Bunsenges. Phys. Chem.* **92**, 68–73.
- Larock, R. C., Burns, L. D., Varaprat, S., Russell, C. F., Richardson, J. W., Janakiraman, M. N. & Jacobson, R. A. (1987). *Organometallics*, **6**, 1780–1789.
- Liesegang, J., James, B. D. & Jiang, Z.-T. (1995). *Integr. Ferroelectr.* **9**, 189–198.
- Linden, A., James, B. D., Liesegang, J. & Gonis, N. (1999). *Acta Cryst. B* **55**, 396–409.
- Maciček, J. & Yordanov, A. (1992). *J. Appl. Cryst.* **25**, 73–80.
- Macrae, C. F., Edgington, P. R., McCabe, P., Pidcock, E., Shields, G. P., Taylor, R., Towler, M. & van de Streek, J. (2006). *J. Appl. Cryst.* **39**, 453–457.
- McKinnon, J. J., Jayatilaka, D. & Spackman, M. A. (2007). *Chem. Commun.* pp. 3814–3816.
- Mitsui, T. & Nakamura, E. (1990). Editors. *Ferroelectrics and Related Substances. Landolt-Börnstein: Numerical Data and Functional Relationships in Science and Technology, New Series III: Crystal and Solid State Physics*, **28B**, §43. Berlin: Springer-Verlag.

- Mitzi, D. B. (2001). *Chem. Mater.* **13**, 3283–3298.
- Morris, R. E. & Wheatley, P. A. (2008). *Angew. Chem. Int. Ed.* **47**, 4966–4981.
- Mustaqim, R. M., Ali, S., Razak, I. A., Fun, H.-K., Goswami, S. & Adak, A. (2005). *Acta Cryst. E61*, o3733–o3734.
- North, A. C. T., Phillips, D. C. & Mathews, F. S. (1968). *Acta Cryst. A24*, 351–359.
- Ohms, U. & Guth, H. (1984). *Z. Kristallogr. New Cryst. Struct.* **166**, 213–217.
- Prince, B. J., Turnbull, M. M. & Willett, R. D. (2003). *J. Coord. Chem.* **56**, 441–452.
- Rabu, P., Rueff, J. M., Huang, Z. L., Angelov, S., Souletie, J. & Drillon, M. (2001). *Polyhedron*, **20**, 1677–1685.
- Rosencher, E. & Vinter, B. (2002). *Optoelectronics*. Cambridge University Press.
- Sheldrick, G. M. (2015a). *Acta Cryst. A71*, 3–8.
- Sheldrick, G. M. (2015b). *Acta Cryst. C71*, 3–8.
- Sørensen, G. O., Mahler, L. & Rastrup-Andersen, N. (1974). *J. Mol. Struct.* **20**, 119–126.
- Spackman, M. A. & Jayatilaka, D. (2009). *CrystEngComm*, **11**, 19–32.
- Sumanesh, Awasthi, A. & Gupta, P. (2016). *Chem Sci Trans*, **5**, 311–320.
- Turner, M. J., McKinnon, J. J., Wolff, S. K., Grimwood, D. J., Spackman, P. R., Jayatilaka, D. & Spackman, M. A. (2017). *CrystalExplorer17*. University of Western Australia.
- Wang, S. D., Herbette, L. G. & Rhodes, D. G. (1989). *Acta Cryst. C45*, 1748–1751.
- Wei, K., Zhang, B., Ni, J., Geng, J., Zhang, J., Xu, D., Cui, Y. & Liu, Y. (2015). *Inorg. Chem. Commun.* **51**, 103–105.
- Westrip, S. P. (2010). *J. Appl. Cryst.* **43**, 920–925.
- White, J. G. (1963). *Acta Cryst.* **16**, 397–403.
- Zabel, M., Pavlovskii, I. & Poznyak, A. L. (2008). *J. Struct. Chem.* **49**, 758–761.

# supporting information

*Acta Cryst.* (2019). E75, 1600-1606 [https://doi.org/10.1107/S2056989019013124]

## Crystal structure, Hirshfeld surface analysis and physicochemical characterization of bis[4-(dimethylamino)pyridinium] di- $\mu$ -chlorido-bis[dichloridomercurate(II)]

Fatma Garci, Hela Ferjani, Hammouda Chebbi, Mariem Ben Jomaa and Mohamed Faouzi Zid

### Computing details

Data collection: CAD-4 EXPRESS (Duisenberg, 1992; Macíček & Yordanov, 1992); cell refinement: CAD-4 EXPRESS (Duisenberg, 1992 ; Macíček & Yordanov, 1992); data reduction: XCAD4 (Harms & Wocadlo, 1995); program(s) used to solve structure: SHELXT2018 (Sheldrick, 2015a); program(s) used to refine structure: SHELXL2018 (Sheldrick, 2015b); molecular graphics: DIAMOND (Brandenburg, 2006) and Mercury (Macrae *et al.*, 2006); software used to prepare material for publication: WinGX (Farrugia, 2012) and publCIF (Westrip, 2010).

### Bis[4-(dimethylamino)pyridinium] di- $\mu$ -chlorido-bis[dichloridomercurate(II)]

#### Crystal data

(C <sub>7</sub> H <sub>11</sub> N <sub>2</sub> ) <sub>2</sub> [Hg <sub>2</sub> Cl <sub>6</sub> ]	Z = 2
M <sub>r</sub> = 860.23	F(000) = 792
Triclinic, P $\bar{1}$	D <sub>x</sub> = 2.454 Mg m <sup>-3</sup>
a = 7.6558 (3) Å	Mo K $\alpha$ radiation, $\lambda$ = 0.71073 Å
b = 11.8961 (5) Å	Cell parameters from 25 reflections
c = 13.5853 (4) Å	$\theta$ = 10–15°
$\alpha$ = 82.950 (3)°	$\mu$ = 13.87 mm <sup>-1</sup>
$\beta$ = 76.072 (3)°	T = 293 K
$\gamma$ = 76.339 (4)°	Parallelepiped, colorless
V = 1164.07 (8) Å <sup>3</sup>	0.72 × 0.24 × 0.18 mm

#### Data collection

Enraf–Nonius CAD-4	5875 independent reflections
diffractometer	3913 reflections with $I > 2\sigma(I)$
Radiation source: fine-focus sealed tube	$R_{\text{int}} = 0.040$
Graphite monochromator	$\theta_{\text{max}} = 28.5^\circ$ , $\theta_{\text{min}} = 2.3^\circ$
$\omega/2\theta$ scans	$h = -10 \rightarrow 2$
Absorption correction: $\psi$ scan	$k = -15 \rightarrow 15$
(North <i>et al.</i> , 1968)	$l = -18 \rightarrow 18$
$T_{\text{min}} = 0.53$ , $T_{\text{max}} = 0.99$	2 standard reflections every 120 reflections
7139 measured reflections	intensity decay: 1%

#### Refinement

Refinement on $F^2$	S = 1.03
Least-squares matrix: full	5875 reflections
$R[F^2 > 2\sigma(F^2)] = 0.055$	236 parameters
wR( $F^2$ ) = 0.153	0 restraints

Hydrogen site location: inferred from neighbouring sites

H-atom parameters constrained

$$w = 1/[\sigma^2(F_o^2) + (0.0933P)^2]$$

$$\text{where } P = (F_o^2 + 2F_c^2)/3$$

$$(\Delta/\sigma)_{\max} = 0.001$$

$$\Delta\rho_{\max} = 3.41 \text{ e \AA}^{-3}$$

$$\Delta\rho_{\min} = -3.00 \text{ e \AA}^{-3}$$

Extinction correction: SHELXL2018

(Sheldrick, 2015b),

$$Fc^* = kFc[1 + 0.001xFc^2\lambda^3/\sin(2\theta)]^{-1/4}$$

Extinction coefficient: 0.0058 (5)

### Special details

**Geometry.** All esds (except the esd in the dihedral angle between two l.s. planes) are estimated using the full covariance matrix. The cell esds are taken into account individually in the estimation of esds in distances, angles and torsion angles; correlations between esds in cell parameters are only used when they are defined by crystal symmetry. An approximate (isotropic) treatment of cell esds is used for estimating esds involving l.s. planes.

### Fractional atomic coordinates and isotropic or equivalent isotropic displacement parameters ( $\text{\AA}^2$ )

	<i>x</i>	<i>y</i>	<i>z</i>	$U_{\text{iso}}^*/U_{\text{eq}}$
Hg1	0.73846 (6)	0.52983 (3)	0.96401 (3)	0.04867 (15)
Hg2	0.70787 (6)	0.02376 (3)	0.53548 (3)	0.05017 (16)
Cl3	0.7012 (4)	0.6752 (2)	0.82926 (18)	0.0507 (6)
Cl5	0.5562 (4)	0.1596 (2)	0.66140 (18)	0.0518 (6)
Cl2	0.4827 (3)	0.5982 (2)	1.11547 (17)	0.0489 (6)
Cl6	0.5814 (4)	0.1067 (2)	0.37887 (17)	0.0487 (5)
Cl1	0.9450 (4)	0.3586 (2)	1.0069 (2)	0.0507 (6)
Cl4	0.9497 (4)	-0.1420 (2)	0.5038 (2)	0.0544 (6)
N1B	0.3722 (13)	0.0129 (9)	0.8551 (6)	0.055 (2)
H1B	0.423341	0.022921	0.791911	0.067*
N1A	0.6907 (12)	0.5280 (8)	0.6462 (6)	0.047 (2)
H1A	0.665775	0.537818	0.710142	0.056*
N2B	0.1208 (12)	-0.0324 (7)	1.1557 (6)	0.0441 (18)
C1B	0.2047 (12)	-0.0182 (8)	1.0590 (6)	0.0359 (19)
C5B	0.2580 (14)	0.0880 (8)	1.0172 (8)	0.043 (2)
H5B	0.237846	0.149257	1.057848	0.051*
N2A	0.8004 (12)	0.4827 (8)	0.3413 (6)	0.047 (2)
C2A	0.7198 (13)	0.4105 (8)	0.5161 (8)	0.042 (2)
H2A	0.712530	0.340021	0.496158	0.050*
C4B	0.3388 (16)	0.0977 (10)	0.9166 (9)	0.058 (3)
H4B	0.372259	0.167244	0.889581	0.069*
C1A	0.7683 (12)	0.4958 (8)	0.4424 (6)	0.0352 (18)
C2B	0.2482 (14)	-0.1070 (9)	0.9916 (7)	0.043 (2)
H2B	0.223027	-0.179339	1.015900	0.052*
C3B	0.3261 (15)	-0.0884 (10)	0.8918 (8)	0.052 (3)
H3B	0.347796	-0.147079	0.848196	0.063*
C5A	0.7751 (14)	0.6032 (9)	0.4768 (8)	0.047 (2)
H5A	0.805230	0.663582	0.430389	0.056*
C4A	0.7372 (15)	0.6156 (9)	0.5779 (8)	0.050 (2)
H4A	0.742924	0.684838	0.600944	0.061*
C3A	0.6831 (14)	0.4271 (9)	0.6157 (7)	0.045 (2)
H3A	0.652280	0.368100	0.663649	0.054*
C7B	0.0765 (17)	0.0644 (11)	1.2239 (8)	0.061 (3)

H7Q	0.016344	0.039805	1.290807	0.091*
H7P	0.188302	0.085789	1.227041	0.091*
H7D	-0.003486	0.129990	1.197662	0.091*
C6B	0.0727 (16)	-0.1412 (10)	1.1987 (8)	0.058 (3)
H6Q	0.013266	-0.134628	1.269144	0.087*
H6D	-0.009493	-0.159869	1.162861	0.087*
H6P	0.182338	-0.201411	1.192574	0.087*
C7A	0.8505 (17)	0.5720 (11)	0.2661 (8)	0.063 (3)
H7I	0.867226	0.546304	0.199482	0.094*
H7J	0.754609	0.640812	0.274933	0.094*
H7K	0.963334	0.588643	0.273377	0.094*
C6A	0.8007 (17)	0.3711 (11)	0.3057 (8)	0.065 (3)
H6K	0.825473	0.376560	0.232724	0.097*
H6I	0.894286	0.311834	0.328549	0.097*
H6J	0.682564	0.351849	0.332384	0.097*

*Atomic displacement parameters ( $\text{\AA}^2$ )*

	$U^{11}$	$U^{22}$	$U^{33}$	$U^{12}$	$U^{13}$	$U^{23}$
Hg1	0.0531 (3)	0.0467 (2)	0.0452 (2)	-0.00220 (18)	-0.01806 (17)	-0.00119 (16)
Hg2	0.0507 (3)	0.0470 (3)	0.0479 (2)	-0.00196 (18)	-0.00822 (17)	-0.00665 (17)
Cl3	0.0702 (17)	0.0420 (12)	0.0451 (12)	-0.0111 (11)	-0.0240 (11)	-0.0015 (10)
Cl5	0.0602 (15)	0.0440 (13)	0.0483 (12)	-0.0159 (11)	0.0017 (11)	-0.0101 (10)
Cl2	0.0486 (13)	0.0604 (15)	0.0393 (11)	-0.0136 (11)	-0.0069 (10)	-0.0111 (10)
Cl6	0.0551 (14)	0.0543 (14)	0.0414 (11)	-0.0190 (11)	-0.0166 (10)	0.0044 (10)
C11	0.0547 (14)	0.0363 (11)	0.0709 (16)	-0.0105 (10)	-0.0348 (12)	0.0018 (11)
Cl4	0.0431 (13)	0.0373 (12)	0.0800 (18)	-0.0075 (10)	-0.0079 (12)	-0.0065 (11)
N1B	0.052 (5)	0.072 (7)	0.038 (4)	-0.005 (5)	-0.012 (4)	-0.002 (4)
N1A	0.057 (5)	0.053 (5)	0.034 (4)	-0.016 (4)	-0.011 (4)	-0.006 (4)
N2B	0.049 (5)	0.048 (5)	0.035 (4)	-0.012 (4)	-0.009 (3)	-0.004 (3)
C1B	0.030 (4)	0.043 (5)	0.035 (4)	0.002 (3)	-0.018 (3)	-0.002 (4)
C5B	0.049 (5)	0.028 (4)	0.050 (5)	-0.001 (4)	-0.018 (4)	0.000 (4)
N2A	0.041 (4)	0.067 (6)	0.033 (4)	-0.011 (4)	-0.007 (3)	-0.005 (4)
C2A	0.040 (5)	0.035 (5)	0.053 (5)	-0.006 (4)	-0.015 (4)	-0.007 (4)
C4B	0.050 (6)	0.047 (6)	0.072 (7)	-0.005 (5)	-0.021 (5)	0.017 (5)
C1A	0.031 (4)	0.042 (5)	0.034 (4)	-0.007 (4)	-0.013 (3)	0.001 (4)
C2B	0.046 (5)	0.044 (5)	0.043 (5)	-0.006 (4)	-0.019 (4)	-0.004 (4)
C3B	0.052 (6)	0.061 (7)	0.046 (5)	0.004 (5)	-0.019 (5)	-0.026 (5)
C5A	0.049 (6)	0.043 (5)	0.051 (6)	-0.013 (4)	-0.018 (5)	0.003 (4)
C4A	0.053 (6)	0.038 (5)	0.061 (6)	-0.004 (4)	-0.013 (5)	-0.014 (5)
C3A	0.046 (5)	0.048 (6)	0.041 (5)	-0.013 (4)	-0.008 (4)	0.004 (4)
C7B	0.061 (7)	0.080 (8)	0.042 (5)	-0.014 (6)	-0.008 (5)	-0.019 (5)
C6B	0.064 (7)	0.063 (7)	0.051 (6)	-0.019 (6)	-0.019 (5)	0.005 (5)
C7A	0.066 (7)	0.074 (8)	0.041 (5)	-0.013 (6)	-0.006 (5)	0.013 (5)
C6A	0.068 (8)	0.081 (9)	0.048 (6)	-0.014 (7)	-0.011 (5)	-0.020 (6)

Geometric parameters ( $\text{\AA}$ ,  $^{\circ}$ )

Hg1—Cl1	2.371 (2)	C2A—C3A	1.344 (14)
Hg1—Cl3	2.380 (2)	C2A—C1A	1.386 (13)
Hg1—Cl2	2.539 (2)	C2A—H2A	0.9300
Hg1—Cl2 <sup>i</sup>	2.975 (2)	C4B—H4B	0.9300
Hg2—Cl4	2.367 (3)	C1A—C5A	1.429 (13)
Hg2—Cl5	2.392 (2)	C2B—C3B	1.357 (15)
Hg2—Cl6	2.542 (2)	C2B—H2B	0.9300
Hg2—Cl6 <sup>ii</sup>	2.934 (3)	C3B—H3B	0.9300
N1B—C4B	1.329 (15)	C5A—C4A	1.352 (15)
N1B—C3B	1.340 (15)	C5A—H5A	0.9300
N1B—H1B	0.8600	C4A—H4A	0.9300
N1A—C3A	1.334 (13)	C3A—H3A	0.9300
N1A—C4A	1.362 (14)	C7B—H7Q	0.9600
N1A—H1A	0.8600	C7B—H7P	0.9600
N2B—C1B	1.326 (12)	C7B—H7D	0.9600
N2B—C6B	1.445 (14)	C6B—H6Q	0.9600
N2B—C7B	1.492 (13)	C6B—H6D	0.9600
C1B—C2B	1.410 (13)	C6B—H6P	0.9600
C1B—C5B	1.429 (14)	C7A—H7I	0.9600
C5B—C4B	1.360 (15)	C7A—H7J	0.9600
C5B—H5B	0.9300	C7A—H7K	0.9600
N2A—C1A	1.357 (11)	C6A—H6K	0.9600
N2A—C7A	1.435 (14)	C6A—H6I	0.9600
N2A—C6A	1.468 (15)	C6A—H6J	0.9600
Cl1—Hg1—Cl3	141.44 (10)	C2A—C1A—C5A	117.1 (8)
Cl1—Hg1—Cl2	112.01 (9)	C3B—C2B—C1B	121.0 (10)
Cl3—Hg1—Cl2	106.16 (9)	C3B—C2B—H2B	119.5
Cl1—Hg1—Cl2 <sup>i</sup>	93.63 (8)	C1B—C2B—H2B	119.5
Cl3—Hg1—Cl2 <sup>i</sup>	88.63 (8)	N1B—C3B—C2B	121.1 (9)
Cl2—Hg1—Cl2 <sup>i</sup>	94.45 (7)	N1B—C3B—H3B	119.4
Cl4—Hg2—Cl5	141.70 (10)	C2B—C3B—H3B	119.4
Cl4—Hg2—Cl6	112.72 (10)	C4A—C5A—C1A	119.1 (10)
Cl5—Hg2—Cl6	105.06 (9)	C4A—C5A—H5A	120.5
Cl4—Hg2—Cl6 <sup>ii</sup>	95.28 (8)	C1A—C5A—H5A	120.5
Cl5—Hg2—Cl6 <sup>ii</sup>	87.53 (8)	C5A—C4A—N1A	120.7 (9)
Cl6—Hg2—Cl6 <sup>ii</sup>	94.73 (7)	C5A—C4A—H4A	119.6
Hg1—Cl2—Hg1 <sup>i</sup>	85.55 (7)	N1A—C4A—H4A	119.6
Hg2—Cl6—Hg2 <sup>ii</sup>	85.27 (7)	N1A—C3A—C2A	120.3 (9)
C4B—N1B—C3B	119.8 (9)	N1A—C3A—H3A	119.9
C4B—N1B—H1B	120.1	C2A—C3A—H3A	119.9
C3B—N1B—H1B	120.1	N2B—C7B—H7Q	109.5
C3A—N1A—C4A	121.2 (8)	N2B—C7B—H7P	109.5
C3A—N1A—H1A	119.4	H7Q—C7B—H7P	109.5
C4A—N1A—H1A	119.4	N2B—C7B—H7D	109.5
C1B—N2B—C6B	121.7 (9)	H7Q—C7B—H7D	109.5

C1B—N2B—C7B	120.2 (9)	H7P—C7B—H7D	109.5
C6B—N2B—C7B	118.1 (8)	N2B—C6B—H6Q	109.5
N2B—C1B—C2B	122.2 (9)	N2B—C6B—H6D	109.5
N2B—C1B—C5B	121.8 (9)	H6Q—C6B—H6D	109.5
C2B—C1B—C5B	116.1 (9)	N2B—C6B—H6P	109.5
C4B—C5B—C1B	118.6 (9)	H6Q—C6B—H6P	109.5
C4B—C5B—H5B	120.7	H6D—C6B—H6P	109.5
C1B—C5B—H5B	120.7	N2A—C7A—H7I	109.5
C1A—N2A—C7A	122.1 (9)	N2A—C7A—H7J	109.5
C1A—N2A—C6A	120.1 (9)	H7I—C7A—H7J	109.5
C7A—N2A—C6A	117.6 (9)	N2A—C7A—H7K	109.5
C3A—C2A—C1A	121.6 (9)	H7I—C7A—H7K	109.5
C3A—C2A—H2A	119.2	H7J—C7A—H7K	109.5
C1A—C2A—H2A	119.2	N2A—C6A—H6K	109.5
N1B—C4B—C5B	123.3 (11)	N2A—C6A—H6I	109.5
N1B—C4B—H4B	118.4	H6K—C6A—H6I	109.5
C5B—C4B—H4B	118.4	N2A—C6A—H6J	109.5
N2A—C1A—C2A	122.8 (9)	H6K—C6A—H6J	109.5
N2A—C1A—C5A	120.0 (9)	H6I—C6A—H6J	109.5

Symmetry codes: (i)  $-x+1, -y+1, -z+2$ ; (ii)  $-x+1, -y, -z+1$ .

#### Hydrogen-bond geometry ( $\text{\AA}$ , $^\circ$ )

$D\text{—H}\cdots A$	$D\text{—H}$	$H\cdots A$	$D\cdots A$	$D\text{—H}\cdots A$
N1A—H1A…Cl3	0.86	2.54	3.239 (8)	140
N1B—H1B…Cl5	0.86	2.46	3.195 (10)	145
C2B—H2B…Cl1 <sup>iii</sup>	0.93	2.82	3.634 (11)	147
C3A—H3A…Cl5	0.93	2.75	3.485 (11)	136

Symmetry code: (iii)  $-x+1, -y, -z+2$ .